Analysis of the all-electrical automatic gain control of travelling-wave semiconductor laser amplifiers

R. Hui
I. Maio
I. Montrosset

Indexing terms: Automatic gain control, Travelling wave, Semiconductor laser amplifier

Abstract: The all-electric automatic gain control of a travelling wave semiconductor laser amplifier through the error signal detected from its junction voltage is analysed. Three different control schemes are compared. The ability to suppress the optical gain variation caused by the polarisation fluctuation is particularly addressed.

1 Introduction

Semiconductor laser amplifiers have been subject of great interest for several years now. Travelling wave semiconductor laser amplifiers have recently been implemented in optical fibre communication systems as optical repeaters and optical preamplifiers. Automatic gain control (AGC) of laser amplifiers is required in more reliable optical communication systems to compensate for the effect related to the drift in the signal polarisation, the input power, the temperature and the device aging.

Intuitively, the actual optical gain of an amplifier can be obtained by extracting fractions of its input and output signals and comparing their power values. The signal proportional to the actual gain can then be compared to a reference value in a differential amplifier, and eventually the resulting error signal can be used to control the bias current of the laser amplifier. Both automatic gain and power control can be performed in this way [1]. However, this method requires two directional couplers inserted in the optical transmission line and two photo detectors for the signal detection. It is somewhat complicated especially in systems with two or more laser amplifiers.

The AGC method proposed [2] would appear more simple. It extracts error signal information from the junction electric voltage of the amplifier because the junction voltage is related to the optical power through the carrier density. However, since the junction voltage also contains the voltage drop across the junction ohm resistance, which is temperature dependent and even larger than the useful signal voltage, a pilot tone has to be applied on the input optical signal in order to increase the sensitivity. Very recently, a new scheme that makes use of a multi-electrode laser has been realised experimentally to monitor the optical gain [3]. In this work, we analyse these schemes in more detail using a nonlinear rate equation model, and a performance comparison is made between them.

2 Theoretical model

The AGC method analysed in this work is based on the fact that the junction electric voltage of a semiconductor laser amplifier is directly related to the carrier density inside the active region. The physical origin of this relationship is attributed to the changes in the quasi-Fermi levels caused by the carrier density changes. Since output power changes modify the value of the carrier density in the device, the junction voltage must be a function of the device gain.

The relation between the junction electric voltage and the carrier density can be expressed by the following integral formula:

$$V_J = V_{J0} - \int_{N_0}^{N} C(N')\,dN' \tag{1}$$

where $C = dV/dN$ [4] determines the sensitivity of the AGC scheme and is analysed in more detail in Appendix 6, N_0, V_{J0} are reference carrier density and the junction voltage at the reference carrier density, respectively. To use the junction voltage to assess the device gain, however, two effects must be allowed for. First, in a travelling wave amplifier the carrier density is a function of the longitudinal position (so $V_J = V_J(z)$) and, secondly, only the electrode voltage V_e can be directly detected (which is independent of z and includes the voltage drop across the semiconductor resistance). We computed the electrode voltage corresponding to a given junction voltage distribution through the device electric equivalent circuit of Fig. 1 where we supposed the device segmented in n longitudinal cells of length $\Delta z = L/n$ and each equivalent circuit bridge represents a cell. The ith voltage generator is set to the junction voltage value $V_J(z_i)$ at the ith cell. Considering a smooth profile of the junction voltage, in Fig. 1 we neglected the longitudinal conductivity, which implies the assumption of only a vertical current flow. In the circuit of Fig. 1, V_e can be determined

This work was supported by European Institute of Technology and Camera di Commercio di Torino under Research Grant on All-Optical Communication Networks and MURST.

Paper 9846J (E3), first received 6th July 1992 and in final revised form 6th September 1993

The authors are with the Dipartimento di Elettronica, Politecnico, Corso Duca degli Abruzzi 24 — 10129 Torino — Italy

by the Millman theorem:

$$V_e = \frac{I + \sum_{i=1}^{n} \frac{V_J(z_i)}{R_i}}{\sum_{i=1}^{n} \frac{1}{R_i}} \tag{2}$$

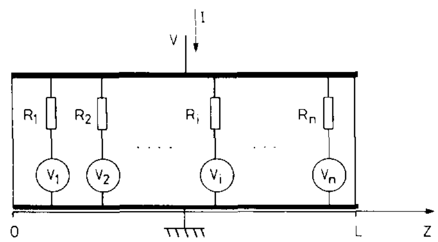

Fig. 1 *Equivalent electric circuit of laser amplifier*

Finally, setting $R_i = nR$ for each i, where R is the total device resistance, the electrode voltage can be written as

$$V_e = RI + \frac{1}{L}\int_0^L V_J(z)\,dz \tag{3}$$

The useful part of V_e is only the term $V_{ave} = (1/L)\int_0^L V_J(z)\,dz$, which is related to the optical power through the carrier density. This term is usually of the same order as the RI term. Meanwhile, the value RI is, in general, junction temperature dependent, so that a pilot tone on the input optical signal is usually required to distinguish the useful signal from RI.

To evaluate V_{ave} as a function of the injection parameter (the unsaturated carrier density) and of the input and output powers (or equivalently of the input power and the actual gain), the carrier density longitudinal profile must be determined.

Generally, both the semiconductor gain and the recombination rate are nonlinear functions of carrier density N. The modal gain can then be expressed as:

$$g_m(N, z) = \Gamma g(N, z) - \alpha \tag{4}$$

where $g(N, z)$ is the material gain, which is nonlinearly related to the carrier density [5], α is the loss coefficient and Γ is the field confinement factor. $g(N)$ has been obtained by cubic spline interpolation of numerical results calculated from semiconductor band theory; as a good approximation, these results can be formulated with the following expressions [6]: $g(\omega, N) = g_p - \gamma_g(\omega - \omega_p)^2$, with $g_p = a_g + b_g N$, $\omega_p = a_p + b_p N$ and $\gamma_g = \alpha_g N^{\beta_g}$.

Neglecting the longitudinal carrier diffusion [5], the stationary carrier rate equation is

$$r(N) + \Gamma_g(N)\frac{P}{\hbar\omega A} = \frac{J}{et} \tag{5}$$

where $r(N) = N/\tau + BN^2 + CN^3$ is the nonlinear carrier recombination rate ($1/\tau$, B and C are the radiative, nonradiative and Auger recombination coefficients, respectively), $\hbar\omega$ the photon energy, P the optical power flux, A the active area, J the injected current density, e the electron charge, and t the active layer thickness.

The rate equation has been normalised to a simple form:

$$\mathscr{R}(N) + \Gamma G(N)p = JK \tag{6}$$

where $\mathscr{R}(N) = r(N)\tau_d$, $G(N) = g(N)/a$, $p = P/P_r$, $P_r = (\omega A)/(a\tau_d)$, $K = \tau_d/(et)$, $a = \partial g/\partial n|_{N=N_s}$ and $1/\tau_d = \partial r/\partial N|_{N=N_s}$. N_s is the unsaturated carrier density value.

The travelling wave equation for the optical power along the longitudinal direction is

$$\frac{dp}{dz} = [\Gamma a G(N) - \alpha]p \tag{7}$$

and the boundary condition at the left facet is

$$p(0) = P(0)/P_r \tag{8}$$

For usual linear gain and recombination, the solution of eqns. 6 and 7 can be easily obtained by computing the $G[N(P)]$ function from eqn. 6 and by integrating eqn. 7. With the nonlinear gain and recombination functions used here, however, the evaluation of the carrier density corresponding to a given optical power from eqn. 6 requires the solution of a nonlinear equation. On the other hand in eqn. 6 p can be obtained as a function of N immediately and therefore, it is computationally convenient to integrate the differential equation for the carrier profile. Such an equation can be obtained from eqn. 7 by replacing dp/dz with $dp/dN \times dN/dz$ and computing dp/dN from eqn. 6:

$$\frac{dN}{dz} = \Gamma a G(N) \Bigg/ \left[\frac{d\mathscr{R}/dN}{\mathscr{R} - JK} - \frac{dG(N)/dN}{G(N)}\right] \tag{9}$$

The unwanted modal gain variations caused by polarisation fluctuations can be taken into account by using for Γ an effective confinement factor determined by the power partition on the two polarisations: $\Gamma = (\Gamma_{TE}P_{TE} + \Gamma_{TM}P_{TM})/(P_{TE} + P_{TM})$. It is also noticed that, unlike another AGC scheme [1] in which the output optical power is detected, the effect of amplified spontaneous emission (ASE) is negligible here because the ASE gives a quasihomogeneous contribution to the carrier density along the devices longitudinal direction.

The z-dependent junction electric voltage can be obtained by the following numerical procedure using eqns. 1–9. With a given input power $P(0)$ and a given polarisation state, the normalised input optical power $p(0) = P(0)/P_r$ can be obtained. Then one can evaluate the carrier density $N(0)$ at $z = 0$ from eqn. 6 with $p = p(0)$. The carrier density profile $N(z)$ can thus be calculated through the numerical integration of eqn. 9 and, once $N(z)$ is known, the output optical power P_{out} and the junction electric voltage V can be obtained from eqns. 7 and 3, respectively.

The numerical parameter values used in the simulation, for the operating wavelength of 1.3 μm, are: $a_g = -0.513 \times 10^3\ \text{cm}^{-1}$, $b_g = 0.356 \times 10^{-15}\ \text{cm}^2$, $a_p = 0.116 \times 10^{16}$ rad/s, $b_p = 0.217 \times 10^{-4}\ \text{cm}^3$ rad/s, $1/\tau = 10^{-9}\ \text{s}^{-1}\ \text{cm}^3$, $B = 8.6 \times 10^{-11}\ \text{s}^{-1}\ \text{cm}^6$, $C = 2 \times 10^{-29}\ \text{s}^{-1}\ \text{cm}^9$, $\alpha = 24\ \text{cm}^{-1}$, $A = 6 \times 10^{-9}\ \text{cm}^2$, $N_s = 3 \times 10^{18}\ \text{cm}^{-3}$, $\Gamma_{TE} = 0.3$ and $\Gamma_{TM} = 0.24$. For N and ω expressed in cm^{-3} and rad/s, respectively $\beta_g = -0.6221$ and $\alpha_g = 0.192 \times 10^{-13}$.

3 Results and discussion

The junction electric voltage signal used in the AGC scheme was first reported in Reference 2. In this case, the junction voltage is

$$V_e = RI + \frac{1}{L}\int_0^L V_J(z)(1 + \delta\cos\Omega t)\,dz \tag{10}$$

where a low frequency pilot tone, with modulation index δ and angular frequency Ω, was applied to the input optical signal, and only the junction electric voltage signal at the frequency of the pilot tone, $v_e = (\delta/L) \int_0^L V_j(z)\, dz$, was detected and used to control the device gain. In the ideally controlled condition, the junction voltage signal is kept constant and any variation in this voltage signal is supposed to be compensated by the feedback control in the injection current. The calculated result reveals that, even in this ideally controlled condition, a small amount of optical gain variation caused by the polarisation variation is still present. The reason for this residual error is explained in Fig. 2, in which the junction

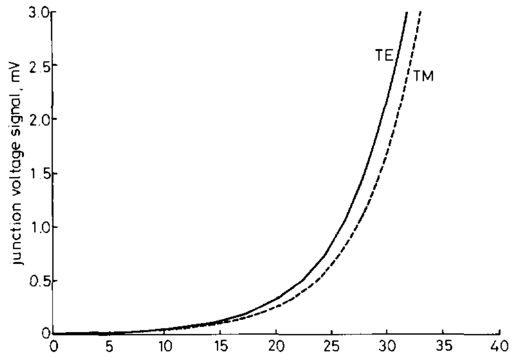

Fig. 2 *Junction electric voltage signal versus optical gain for pure TE mode (solid line) and pure TM mode (dashed line)*

Normalised input optical power = 20 dBm; modulation index of pilot tone = 0.1

electric voltage signal versus device optical gain is plotted for *TE* (solid line) and *TM* (dashed line) polarisations. Since the confinement factor for the *TM* wave is smaller than that of the *TE* wave, the saturation optical power is higher, and thus less saturation is expected for *TM* wave, so that the junction voltage signal is smaller than that for *TE* wave. In ideally controlled conditions, the optical gain variation caused by the polarisation variation between *TE* and *TM* mode is shown in Fig. 3 with

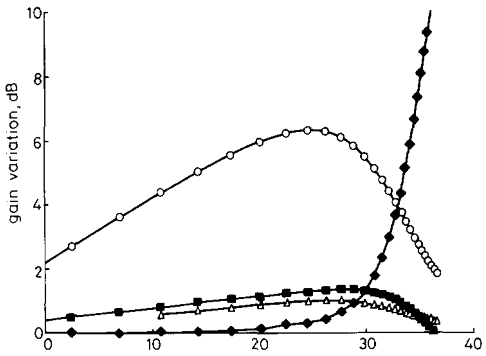

Fig. 3 *Residual optical gain variation caused by polarisation change versus optical gain for different AGC schemes*

Empty triangles: single electrode, with pilot tone; solid rectangles: three electrodes, without pilot tone; solid diamonds: three electrodes, with pilot tone; empty circles: without control; normalised input optical power = −20 dBm; modulation index of pilot tone = 0.1

empty triangles. This residual error depends on the difference of the confinement factor between *TE* and *TM* modes. As a reference, the optical gain variation caused by the polarisation change without AGC is also plotted in the same Figure in empty circles. In this AGC scheme, the optical gain variation can be suppressed by about 5 times.

An alternative AGC structure uses a multielectrode laser amplifier. The basic idea is to take advantage of the fact that the photon distribution along the longitudinal direction of the laser amplifier is not uniform and this nonuniformity is related to the light amplification. A typical junction electric voltage variation profile along the longitudinal direction of a laser amplifier is shown in Fig. 4 for TE and TM polarised input light. However, the

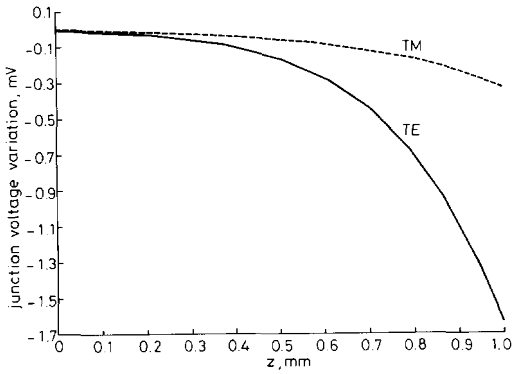

Fig. 4 *Junction voltage variation profile along device longitudinal direction for TE mode (solid line) and TM mode (dashed line)*

Normalised input optical power = −20 dBm; optical gain for TE mode = 20 dB; for TM mode is 14 dB

conductivity of the electrode has the effect of averaging the voltage along the length covered by the electrode as analysed before, so that the voltage variation along the cavity length is not detectable except when a multielectrode TWA is used as schematically shown in Fig. 5.

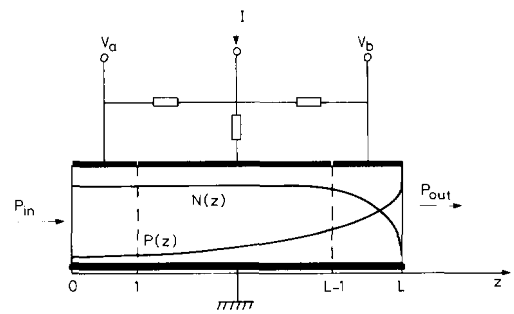

Fig. 5 *Laser amplifier with three electrodes*

If we consider the material of the laser amplifier uniform in the longitudinal direction, the electric voltages of the first and the third electrode are, respectively:

$$V_a = RIl_1/L + \frac{1}{l_1}\int_0^{l_1} V_j(z)(1 + \delta \cos \Omega t)\, dz \tag{11}$$

$$V_b = RIl_2/L + \frac{1}{l_2}\int_{L-l_2}^{L} V_j(z)(1 + \delta \cos \Omega t)\, dz \tag{12}$$

The advantage of using a short electrode at the end of the device to detect the voltage signal has been demonstrated to increase the detection sensitivity [7]. A recent paper reported a method to monitor the optical gain through the junction electric voltage signal of a three-section TWA. Where the pilot tone was used in the input optical signal, the voltage signal ratio v_b/v_a versus the device optical gain was found to have a linear relationship in the logarithm scale, where v_a and v_b are the AC part of V_a and V_b, respectively. In our nonlinear model, this characteristic is examined and reported in Fig. 6, where the

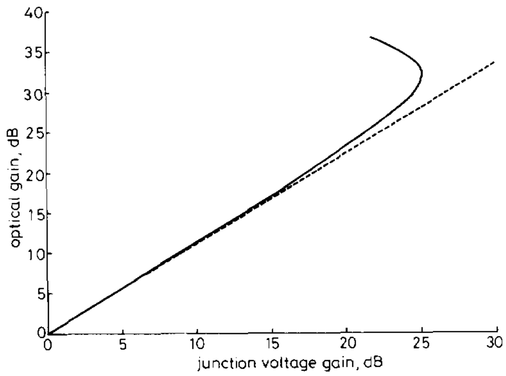

Fig. 6 *Optical gain versus junction voltage gain in three-electrode device with pilot tone (solid line)*

Normalised input optical power = −20 dBm; dashed line is obtained through linear theory

total cavity length is 1 mm and the two signal electrodes are chosen with the same length $l_1 = l_2 = 0.1$ mm. The result calculated in the linear approximation [3] is also plotted in the same Figure. Agreement is good except for the high gain regime where nonlinear effect becomes important. If this detected junction voltage signal is used to perform the automatic gain control to suppress the optical gain variation caused by the input polarisation change, the residual error in the 'ideally' controlled condition is plotted in Fig. 3 in solid diamonds. In the case where the optical gain is less than 20 dB, the residual error is less than 0.2 dB, however, the AGC performance is seriously degraded when the optical gain reaches up to 30 dB in the highly nonlinear regime.

It is noticed that, in the above AGC scheme, a pilot tone is used in the input optical signal. This will pose the inconvenience at the transmitter part, and thus reduce the feasibility of the AGC application. For the first AGC scheme (i.e. in the laser amplifier of one electrode), the pilot tone is not available because of the junction DC Ohm resistance. However, if the multielectrode laser amplifier is used, as in the case of Fig. 4, the junction electric voltage difference between the two terminal electrodes, $V_a - V_b$, is independent of the DC ohm resistance if these two sections have the same length. When this DC voltage difference is used as the reference in the AGC system, in the ideally controlled condition, the residual error in the optical gain caused by the polarisation change between TE and TM mode is plotted also in Fig. 3 using solid rectangles. In this case, the control system performance is similar to that of the first scheme (single electrode + pilot tone). Except for excluding the pilot tone, the major advantage, however, is that, using multielectrode laser amplifier, one can have much better sensitivity in detecting voltage signal in comparison to the one electrode case [5].

4 Conclusion

In conclusion, the all-electric automatic gain control of a semiconductor laser amplifier is analysed using the carrier density rate equation in the travelling wave model. Three different control schemes are compared. The ability to suppress the output power variation caused by the polarisation fluctuation is particularly addressed.

5 References

1 ESKILDSEN, L., OLESEN, D.S., MIKKESEN, B., FARRE, J., and STUBKJAER, K.E.: 'Automatic gain and power control of semiconductor laser amplifier'. Proceedings of ECOC '90, 1990, pp. 621–624
2 ELLIS, A., MALYON, D., and STALLARD, W.A.: 'A novel all electrical scheme for laser amplifier gain control'. Proceedings of ECOC '88, 1988, pp. 487–490
3 NEWKIRK, M.A., KOREN, U., MILLER, B.I., CHIEN, M.D., YOUNG, M.G., KOCH, T.L., RAYBON, G., BURRUS, C.A., TELL, B., and BROWN-GOEBELER, K.F.: 'Three-section semiconductor optical amplifier for monitoring of optical gain', *IEEE Photonics Technol. Lett.*, 1992, **4**, (11), pp. 1258–1260
4 MARCUS, D.: 'Heterodyne detection with an injection laser Part I: principle of operation and conversion efficiency', *IEEE J.*, 1990, **QE-26**, (1), pp. 85–93
5 AGRAWAL, G.P., and DUTTA, A.N.: 'Long wavelength semiconductor laser devices' (Van Nostrand Reinhold, New York, 1986)
6 CAPONIO, N.P., GOANO, M., MAIO, I., MELIGA, M., BAVA, G.P., DESTEFANIS, D., and MONTROSSET, I.: 'Analysis and design criteria of three-section DBR tunable lasers', *IEEE J.*, 1990, **SAC-8**, (6), pp. 1203–1212
7 FORTENBERRY, R.M., LOWERY, A.J., and TUCKER, R.S.: 'Up to 16 dB improvement in detected voltage using two-section semiconductor optical amplifier detector', *Electron. Lett.*, 1992, **28**, (5), pp. 474–476

6 Appendix

6.1 Evaluation of the junction voltage sensitivity

The proportionality constant C, appearing in eqns. 6 and 10, is an important factor which is directly related to the sensitivity of the present AGC scheme. The junction electric voltage $V(N)$ is related to the carrier density through quasiFermi levels of electrons and holes μ_n and μ_p by the well known relation [3, 4]:

$$V(N) = \frac{\mu_n - \mu_p}{q} \tag{13}$$

where q is the electron charge and the quasiFermi levels of electrons and holes depend on the carrier density. The differential change in the junction voltage caused by the change of the carrier density can be expressed as follows:

$$C = \frac{1}{q}\left(\frac{\partial \mu_n}{\partial N} - \frac{\partial \mu_p}{\delta N}\right) \tag{14}$$

According to Marcus [4], this relationship can be simplified yielding the following result:

$$C = \frac{kT}{qN}\{[1 + (0.8736 F_p^{2/3})^{1.82}]^{1/1.82} + [1 + (0.8736 F_n^{2/3})^{1.82}]^{1/1.82}\} \tag{15}$$

with

$$F_p = \frac{N}{4\pi}\left(\frac{h^2}{2m_h kT}\right)^{3/2} \tag{16}$$

and

$$F_n = \frac{N}{4\pi}\left(\frac{h^2}{2m_e kT}\right)^{3/2} \tag{17}$$

where, $m_e = 0.07 \times (9.11 \times 10^{-31})$ kg and $m_h = 0.7 \times (9.11 \times 10^{-31})$ kg are the effective mass of electrons and holes respectively, k is the Boltzmann constant, h is the Planck's constant and $T = 300$ K is the absolute temperature.